

Lawrence Berkeley National Laboratory

Lawrence Berkeley National Laboratory

Title

Influence of base and PAG on deprotection blur in EUV photoresists and some thoughts on shot noise

Permalink

<https://escholarship.org/uc/item/27n0b1kh>

Author

Anderson, Christopher N.

Publication Date

2009-03-18

**Influence of base and PAG on deprotection blur in EUV
photoresists and some thoughts on shot noise**

Christopher N. Anderson*

*Applied Science & Technology Graduate Group,
University of California, Berkeley, Berkeley, CA 94720, USA*

Patrick P. Naulleau[†] and Dimitra Niakoula

*Center for X-ray Optics, Lawrence Berkeley National Laboratory,
1 Cyclotron Road, Berkeley, CA 94720, USA*

Elsayed Hassanein and Robert Brainard

College of Nanoscale Science and Engineering, University at Albany, NY 12203

Gregg Gallatin

Applied Math Solutions, LLC

Kim Dean

SEMATECH, Austin, TX 78741

Abstract

A contact-hole deprotection blur metric has been used to monitor the deprotection blur of an experimental open platform resist (EH27) as the weight percent of base and photo acid generator (PAG) were varied. A 6x increase in base weight percent is shown to reduce the size of successfully patterned 1:1 line-space features from 52 nm to 39 nm without changing deprotection blur. Corresponding isolated line-edge-roughness is reduced from 6.9 nm to 4.1 nm. A 2x increase in PAG weight percent is shown to improve 1:1 line-space patterning from 47 nm to 40 nm without changing deprotection blur or isolated LER. A discussion of improved patterning performance as related to shot noise and deprotection blur concludes with a speculation that the spatial distribution of PAG molecules has been playing some role, perhaps a dominant one, in determining the uniformity of photo generated acids in the resists that have been studied.

PACS numbers:

*Electronic address: cnanderson@berkeley.edu

†Also at College of Nanoscale Science and Engineering, University at Albany, NY 12203

I. INTRODUCTION

Resists for extreme ultraviolet (EUV) lithography ($\lambda = 13.5$ nm) are currently being optimized to meet the demanding specifications required beyond the 32 nm manufacturing node. At the present time the interplay between deprotection blur, line-edge-roughness (LER), and other factors contributing to the overall performance of EUV resists is not well understood. In practice, small perturbations in resist or process parameters almost always produce observable changes in printing performance yet the explanations for the observed changes are often speculative at best. In an attempt to better understand EUV resists, and how to improve them, there has been a large effort to develop resist metrics that can deconvolve the effects of deprotection blur, LER and other factors in producing observed performance changes.

Much of the recent effort on resist metrics has been weighted towards developing metrics that can quantify the resolution limits of EUV resists. In a practical sense, resist resolution is often defined as the smallest sized 1:1 features that pattern with an exposure latitude greater than some level. This definition, however, includes effects such as pattern collapse and top loss that may cause the observed resolution to be larger than the actual resolution limit as determined solely by fundamental resist properties. For the purposes of understanding and optimizing resists, it is useful to think of intrinsic resolution as a deprotection blur or a point-spread function (PSF) that represents the fundamental blurring process that occurs during chemical amplification. Over the past four years a variety of approaches have been developed to quantify the deprotection blur in EUV resists: iso-focal bias [1], LER correlation length [2], modulation transfer function (MTF)[3, 4], corner rounding [5, 6], and through-dose contact-hole printing [5–8].

The validity of these approaches has been assessed by comparing their results to observed patterning ability in a large sampling of resists [19]. At the present time, the MTF, corner rounding, and contact-hole metrics have repeatedly shown consistency with direct observation [5, 9]. The contact-hole metric, however, has several properties that currently make it attractive for large-scale resist comparisons: it has very fast turnaround times, it has very little ambiguity in data collection and data analysis [20], it has been well-characterized to measurement uncertainties and it has shown remarkable reproducibility in practice [7].

There have been attempts to develop resist models that describe and predict the effects

of increased base loading on observable characteristics such as LER and patterning ability [10]. It has been speculated that deprotection blur in chemically amplified resists is not directly correlated to the relative concentrations of base or photo acid generator (PAG) in the resist [10]. It is not clear, however, the extent to which changing base and PAG concentrations alters other resist properties (i.e., dissolution, quantum yield, absorptivity, distribution statistics) that also may affect observed printing characteristics. In an attempt to deconvolve the contributions of deprotection blur in observed performance changes through base and PAG loading we use the contact-hole metric to monitor the deprotection blur of EH27 resist [11] as the relative weight percent of base and PAG is varied. We also provide line-space printing data through pitch for each base-PAG combination to correlate changes in observed printing characteristics with changes in measured deprotection blur.

II. THE CONTACT-HOLE DEPROTECTION BLUR METRIC

The contact-hole metric has been described in detail in the literature [6, 7] and is only summarized here. The metric involves capturing scanning electron microscope (SEM) images of contact-holes through dose at best focus in the focus-exposure-matrix (FEM) and measuring the average printed diameter (PD) at each dose. Experimental PD vs. dose data is then compared to modeled PD vs. dose data generated using the HOST PSF resist blur model [13]. Deprotection blur is determined by finding the modeled blur that minimizes the mean-squared-error between the modeled and experimental PD vs. dose data.

As with most PSF-based resolution metrics, the contact-hole metric requires the ability to accurately model the aerial images that create the experimental printing data. In practice, uncertainties in exposure tool aberrations and focus place constraints on the accuracy to which this can be done. The sensitivity of the contact-hole metric to limitations in aerial image modeling has been previously characterized at the SEMATECH Berkeley MET printing facility assuming 0.15 nm RMS errors in interferometrically measured aberrations [12] and assuming 50 nm focus steps in the FEM. The aerial-image-limited error bars in extracted deprotection blur for the contact-hole metric have been reported at 1.25 nm RMS [6].

Several other contact metric error sources have been identified and analyzed in previous work [7]: picking the best-focused row from the FEM, SEM focus, SEM electron beam dosing, and SEM image analysis. The error bars from these sources have been shown to be

the same order as the error-bars due to limitations in aerial image modeling. In addition to this work, a reproducibility experiment has shown that the full-process error bars for the contact-hole metric are within the 1.75 nm quadrature addition of the reported experimental and modeling error-bars [7].

III. EXPERIMENT AND RESULTS

All EH27 resist formulations were prepared at the University at Albany. The resist polymer is 65/20/15 PHS/Sty/TBA, the PAG is DTBP-PFBS, the base is TBAH, and the solvent is 50/50 PMA/Ethyl lactate. Table I summarizes the base/ PAG weight percentages for each formulation and indicates the relative base/PAG weight percent labeling convention used throughout this paper. The resist solid/solvent ratio in weight percent is 5/95 in all samples. In all experiments the resist was spin-coated and softbaked at 130° C for 60 seconds to yield a film thickness of 125 nm on HMDS-primed four inch wafers. Following post-exposure bake at 130° C for 60 seconds, resists were developed using a single puddle of Rohm and Haas MF26A for 45 seconds. All exposures were performed at the 0.3 numerical aperture SEMATECH Berkeley microfield exposure tool printing facility at the Advanced Light Source at Lawrence Berkeley National Laboratory using conventional $\sigma = 0.35 - 0.55$ annular illumination [14]. Line-space and contact-hole data were printed using the LBNL 5,2 dark field and LBNL 7,2 dark field masks, respectively. Contact features for the resolution metric were coded to print with a 50 nm diameter and 125 nm pitch (1:1.5 duty cycle).

All SEM analysis was performed at LBNL on a Hitachi S-4800 with a working distance of 2 mm and an acceleration voltage of 2.0 kV. All line-space and contact-hole data were characterized using offline analysis software [15]. Quoted LER values for line-space printing are 3σ and are the average of the eight central lines in the 10-line patterns (see, for example, Figure 1). PD values used for the contact metric are the average of 25 central contacts captured in a single SEM image. All contact metric error sources identified in previous work have been minimized by adhering to suggested process guidelines [7]: all SEM images are well focused, with emission current fixed throughout each through-dose set; SEM electron beam dosing is avoided by focusing in on a local contact site and shifting the field by 1 μm just before image capture; SEM images are gathered by the same person; and all PD measurements are made at the same threshold level (0.5) in the image analysis software.

We have determined the deprotection blur of EH27 resist with relative base weight percents of 0.33, 0.66, 1.0, 1.5, and 2.0 and relative PAG weight percents of 0.67, 1.0, and 1.33. Figure 1 shows SEM images of bright field 1:1 lines at best focus printed in EH27 resist with different weight percentages of base. Figure 2 shows the corresponding data for the PAG study. These data show that higher levels of base and PAG improve patterning ability and LER at smaller features. We also observe that while increased PAG loading improves nested line performance, the semi-isolated (outer) lines start to fuse at the highest PAG weight percent. Isolated edge LER (or intrinsic LER), which measures the LER in a regime where pattern collapse and other effects cannot dominate line edge formation is determined by measuring the LER of 100 nm 1:1 line-space patterns; the results are summarized in Table II. Through base, intrinsic LER improves while no statistically significant change in intrinsic LER is observed through PAG. The deprotection blurs of the various resists, as determined by the contact-hole metric are also shown in Table II. We observe no statistically significant change in deprotection blur for the EH27 resist through base and PAG levels despite the observed changes in printing performance.

IV. DISCUSSION

Increased levels of base and PAG improve patterning ability in EH27 resist without changing the deprotection blur measured by the contact metric. In addition, increased base weight percents raise the dose required to print 50 nm 1:1 line-space patterns while increased PAG weight percents reduce the dose required to print 50 nm 1:1 line-space patterns (see Table II). Performance improvements with increased base and PAG, correlated to changes in dose-to-size, warrant a discussion of photon arrival statistics and shot noise.

It is very plausible that resist patterning is strongly affected by the spatial distribution of acids that are generated during exposure. As a result, improvements of the signal-to-noise ratio (SNR) [21] of absorbed photons (reductions of shot noise) are often speculated as the leading cause of improved patterning with higher base loading [16, 17]. While these claims are very reasonable, the mechanism relating reduced shot noise to improved patterning is still not completely understood; no experimental data has explicitly shown the relationship between the SNR of absorbed photons and the SNR of photo-generated acids in EUV resists. We do know, however, that in addition to the absorbed photon distribution, the PAG

distribution should also play a role in determining where and how many PAG molecules are activated during exposure.

One would expect that if the SNR of acids was dominated by the SNR of absorbed photons, and not the spatial distribution of the PAG, LER would improve when making the jump from EUV ($\lambda = 13$ nm) to DUV ($\lambda = 248$ nm) printing where there is at least a factor of ten increase in the density of absorbed photons [18]. Two separate experiments, however, have shown that there is no obvious trend toward an increase in EUV LER (relative to that of DUV LER) as resist photospeed is increased [17, 18]. Assuming the results are not determined by image-log slope effects, these data suggest that the acid SNR is not dominated by the absorbed photon SNR. In addition they suggest that improved performance routinely observed [16, 17] at higher base weight percents should not be attributed to reduced shot noise. Moreover, the work here suggests that improved deprotection blur is also not the mechanism behind improved patterning with increased base and PAG.

It is possible that the spatial distribution of PAG and base molecules has largely determined the SNR of photo generated acids in the resists that have been studied. To elucidate, imagine a charge-coupled detector (CCD) where the pixel gain is a function of pixel position in the detector array. Consider a blanket exposure in which we wish to measure the spatial distribution of photon statistics arriving at the CCD. Provided the CCD gain SNR (the ratio of the mean pixel gain and the standard deviation of the pixel gain) is larger than the Poisson-limited SNR of the arriving photons, the statistics of the detected signal will resemble those of the photons. If, however, the CCD gain SNR is quite low, the SNR of the detected signal will be dominated by the non uniformity of the detector and one could be fooled into thinking the photon statistics are very poor. Abstracting the idea of non-uniform CCD gain to photoresist, one can imagine a PAG distribution with a large enough pixel-to-pixel variance in absorption or quantum yield that the PAG SNR actually dominates the SNR of photo-generated acids.

Throughout the PAG series, base weight percent, bake, and development parameters remain fixed so it is very likely that all PAG formulations require close to the same initial quantity of photo-generated acids to print at coded feature sizes. The fact that we observed reduced dose with increased PAG weight percent is a good indicator that each arriving photon is somehow more likely to interact with a PAG when PAG concentration is increased. One possibility is that increased PAG weight percent improves the bulk absorptive properties

of the resist and leaves the quantum yield unaffected. In this case, each absorbed photon would activate the same number of PAG molecules as in the reference formulation (since quantum yield is the same as the reference), however less arriving photons would be required to establish the number of absorbed photons needed for adequate deprotection. On the other hand, it could be that increased PAG does nothing to the bulk absorptive properties of the resist and a lower dose would mean that less photons are absorbed. In this case, each absorbed photon would have to do more work than in the reference formulation, i.e., the quantum yield would have to increase. Of course, some mixture of these two situations could also happen.

In both above arguments the increased PAG weight percent formulation absorbs at most the same number of photons as the reference formulation so one cannot claim that shot noise reductions are responsible for improved patterning ability. If structural effects are ruled out, it is possible that improved PAG distributions are responsible for improved patterning with increased PAG. The situation through base, although not described in detail can be summarized succinctly. Although higher base levels are correlated to increased SNRs of absorbed photons (due to higher doses), it is possible that the increased *signal* of absorbed photons – not the fact that it also becomes relatively less noisy – is what drives an increased acid SRN simply by activating more of the PAG molecules that are there to begin with. If we assume Poisson PAG statistics as an upper limit on PAG uniformity (the statistics may actually be worse), it is not difficult to imagine an increased PAG weight percent or an increased photon signal that enables the PAG molecules that do get activated during exposure to do so in a more uniform fashion.

V. CONCLUSIONS

The size of successfully patterned 1:1 line-space features in EH27 resist is reduced from 51 nm to 39 nm with a 6x increase in base and from 47 nm to 40 nm with a 2x increases in PAG. Isolated edge LER is improved from 6.9 nm to 4.1 nm with a 6x increase in base; no change in intrinsic LER is observed for a 2x increase in PAG. No change in deprotection blur is observed through base and PAG. The results of the PAG study, in combination with previous work on shot noise in EUV resists [17, 18] support the notion that PAG distribution statistics have been playing some role, perhaps a dominant one, in determining

the signal-to-noise ratio of the acid distribution generated during EUV exposures.

VI. ACKNOWLEDGMENTS

The authors are greatly indebted to Paul Denham, Ken Goldberg, Brian Hoef, Gideon Jones, and Jerrin Chiu of the Center for X-Ray Optics at Lawrence Berkeley National Laboratory for expert support with the exposure tool as well as the entire CXRO engineering team for building and maintaining the EUV exposure tool. The authors are grateful for support from the NSF EUV Engineering Research Center. This work was supported by the Director, Office of Science, of the U.S. Department of Energy under Contract No. DE-AC02-05CH11231. This research was also supported by SEMATECH and performed at Lawrence Berkeley National Laboratory using the SEMATECH MET exposure facility at the Advanced Light Source. Lawrence Berkeley National Laboratory is operated under the auspices of the Director, Office of Science, Office of Basic Energy Science, of the US Department of Energy.

-
- [1] G. M. Schmid, M. D. Stewart, C. Wang, B. D. Vogt, M. Vivek, E. K. Lin, C G Willson, "Resolution limitations in chemically amplified photoresist systems," Proc. SPIE 5376, 333-342 (2004).
 - [2] G. F. Lorusso, P. Leunissen, M. Ercken, C Delvaux, F.V. Roey, N. Vandenbroeck, "Spectral analysis of line width roughness and its applications to immersion lithography," J. Microlith., Microfab., Microsyst., 5(2) (2006).
 - [3] J. Hoffnagle, W. D. Hinsberg, F. A. Houle, and M. I. Sanchez, "Characterization of photoresist spatial resolution by interferometric lithography", Proc. SPIE 5038, 464-472 (2003).
 - [4] T. Brunner, C. Fonseca, N. Seong, M. Burkhardt, "Impact of resist blur on MEF, OPC and PD control," Proc. SPIE 5377, (2004)
 - [5] P. Naulleau and C. Anderson "Lithographic metrics for the determination of intrinsic resolution limits in EUV resists," Proc. SPIE 6517, (2007)
 - [6] C. Anderson and P. Naulleau, "Sensitivity study of two high-throughput resolution metrics for photoresists," Appl. Opt. Vol 47, No. 1 (2008).

- [7] C. Anderson and P. Naulleau, “A high-throughput contact-hole resolution metric for photoresists: full-process sensitivity study,” Proc. SPIE 6923 (2008).
- [8] P. Dirsken, J. Braat, A. J.E.M. Janssen, A. Leeuwestein, H. Kwinten, and D. V. Steenwinckel, “Determination of resist parameters using the extended Nijboer-Zernike theory,” Proc. of SPIE 5377 150-159 (2004).
- [9] T. Wallow, R. Kim, B. La Fontaine, P. Naulleau, C. Anderson, R. Sandberg, Progress in EUV Photoresist Technology, Proc SPIE 6533, 653317 (2007)
- [10] G. M. Gallatin, P. Naulleau, D. Niakoula, R. Brainard, E. Hassanein, R. Matyi, J. Thackeray, K. Spear, K. Dean, “Resolution, LER and sensitivity limitations in photoresists,” Proc. SPIE 6921 (2008)
- [11] R. Brainard, E. Hassanein, J. Li, P. Pathak, B. Thiel, F. Cerrina, R. Moore, M. Rodriguez, B. Yakshinskiy, E. Loginova, T. Madey, R. Matyi, M. Malloy, A. Rudack, P. Naulleau, A. Wuest, K. Dean, “Photons, electrons and acid yields in EUV photoresists: a progress report,” Proc. SPIE 6923 (2008)
- [12] K. Goldberg, P. Naulleau, P. Denham, S. Rekawa, K. Jackson, E. Anderson, and J. Alexander Liddle. “At-Wavelength Alignment and Testing of the 0.3 NA MET Optic, J. Vac. Sci. and Technol. B 22, 2956-2961 (2004).
- [13] C. Ahn, H. Kim, and K. Baik, “A novel approximate model for resist process,” Proc. SPIE 3334, 752763 (1998).
- [14] P. Naulleau “Status of EUV micro-exposure capabilities at the ALS using the 0.3-NA MET optic,” Proc. SPIE 5374, 881-891 (2004).
- [15] SuMMIT software is distributed by EUV Technology, Martinez, CA 94553, <http://www.euvl.com/summit>
- [16] D. Steenwinckel, J. Lammers, T. Koehler, R. Brainard, and P. Trefonas, “Resist effects at small pitches,” JVST B 24 (1) Jan/Feb (2006).
- [17] R. Brainard, P. Trefonas, J. Lammers, C. Cutler, J. Mackevich, A. Trefonas, and S. Robertson, “Shot noise, LER and quantum efficiency of EUV photoresists,” Proc. SPIE 5374 (2004).
- [18] P. Dentinger, L. Hunter, D. O’Connell, S. Gunn, D. Goods, T. Fedynyshyn, R. Goodman, and D. Astolfi, “Photospeed considerations for extreme ultraviolet lithography resists,” JVST B 20 (6) (2002).
- [19] Although patterning ability is influenced by factors other than deprotection blur, it is the only

firm footing which exists to judge the validity of the different approaches

- [20] The MTF metric requires one to decide where resist just starts being removed and where resist is just barely cleared; both of these subjective decisions significantly influence the result of the metric.
- [21] By signal-to-noise ratio we mean the ratio of the average number of events per pixel and the standard deviation of the number of events per pixel where a pixel is some space-time volume.

List of Figures

1 Base loading study. Through-pitch SEM images of bright field 1:1 lines printed in EH27 resist. Relative base weight percents are indicated to the left of each row. Half-pitch coded feature sizes are indicated at the bottom of each column. LER information for each SEM image is indicated in the table. 13

2 Photo-acid generator (PAG) study. Through-pitch SEM images of bright field 1:1 lines printed in EH27 resist. Relative PAG weight percents are indicated to the left of each row. Half-pitch coded feature sizes are indicated at the bottom of each column. LER information for each SEM image is indicated in the table. 14

List of Tables

I EH27 resist PAG/base specifications 15

II Base and PAG dependence on deprotection blur and other performance metrics 16

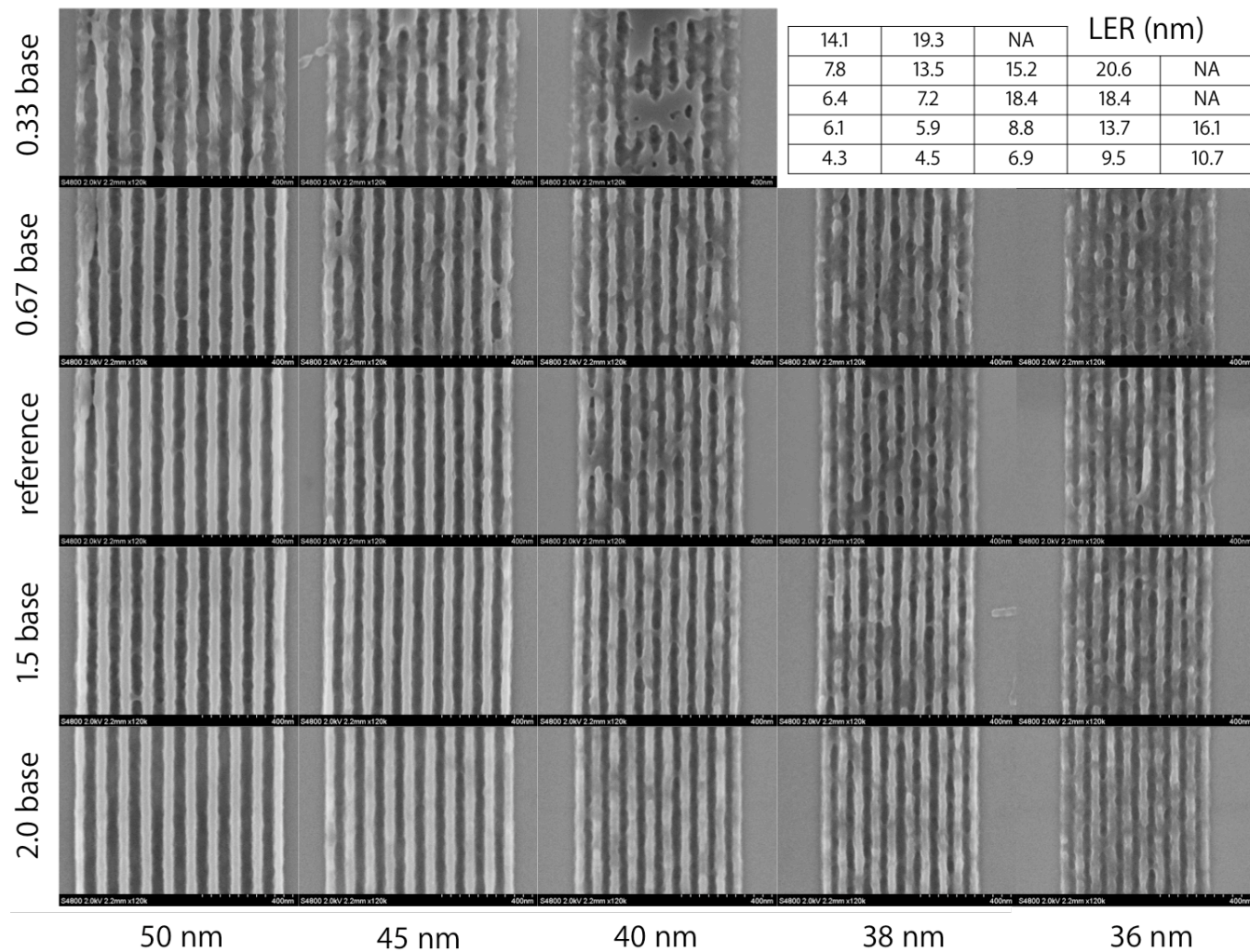


FIG. 1: Base loading study. Through-pitch SEM images of bright field 1:1 lines printed in EH27 resist. Relative base weight percents are indicated to the left of each row. Half-pitch coded feature sizes are indicated at the bottom of each column. LER information for each SEM image is indicated in the table.

				LER (nm)
7.9	10	20.9	NA	
6.4	7.2	18.4	18.4	NA
5.8	7.4	16	15.1	NA

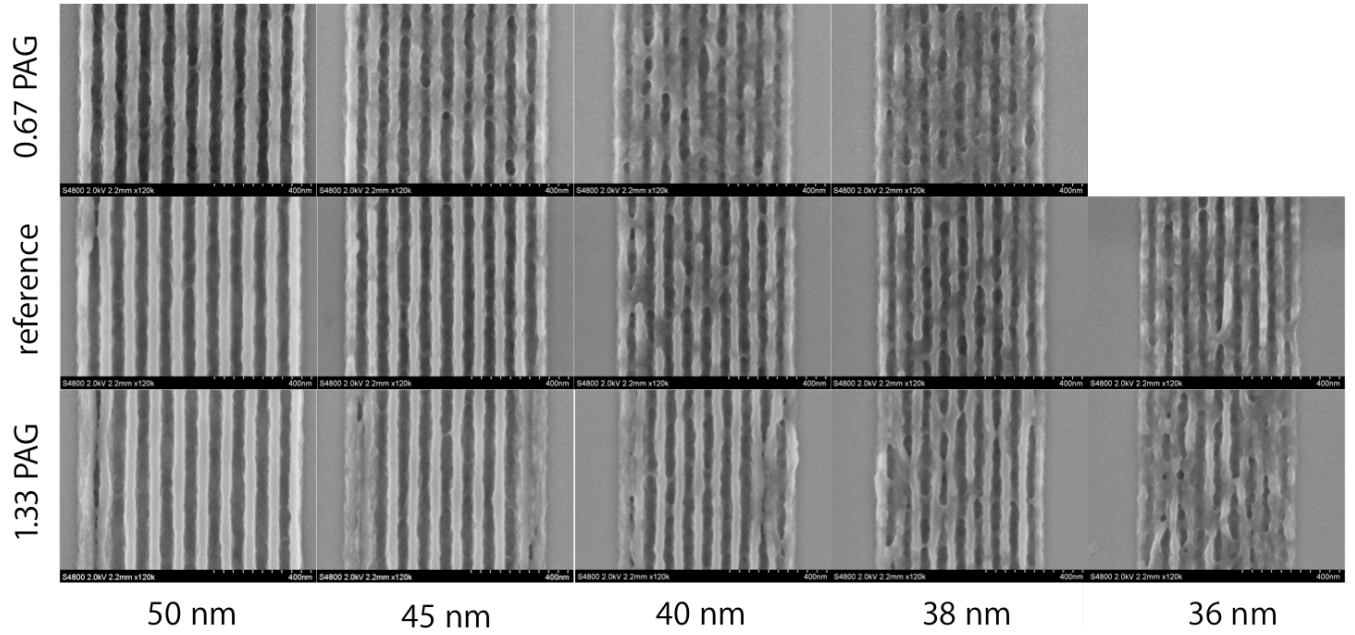


FIG. 2: Photo-acid generator (PAG) study. Through-pitch SEM images of bright field 1:1 lines printed in EH27 resist. Relative PAG weight percents are indicated to the left of each row. Half-pitch coded feature sizes are indicated at the bottom of each column. LER information for each SEM image is indicated in the table.

TABLE I: EH27 resist PAG/base specifications

Resist	PAG % ^a	Base % ^a	Label
EH-27C-103	7.5	0.17	0.33 Base
EH-27D-105	7.5	0.34	0.67 Base
EH-27E-105	7.5	0.50	REF
EH-27F-107	7.5	0.75	1.50 Base
EH-27G-107	7.5	1.00	2.00 Base
EH-27A-103	5.0	0.50	0.67 PAG
EH-27H-109	10.0	0.50	1.33 PAG

^a% is weight percent.

TABLE II: Base and PAG dependence on deprotection blur and other performance metrics

Resist	Label	Deprotection	Patterning	LER (nm)	Isolated LER (nm)	Esize (mJ/cm ²)
		blur (nm)	ability (nm)	50 nm 1:1	100 nm 1:1	
EH-27C-103	0.33 Base	17.0	52	17.0	6.9	1.9
EH-27D-105	0.67 Base	17.3	47	7.2	5.6	3.2
EH-27E-105	REF	16.7	43	6.4	4.7	6.4
EH-27F-107	1.50 Base	15.0	42	6.1	4.9	7.8
EH-27G-107	2.00 Base	17.1	39	4.1	4.1	10.7
EH-27A-103	0.67 PAG	17.0	47	7.4	5.4	6.4
EH-27E-105	REF	16.7	43	6.4	4.7	5.0
EH-27H-109	1.33 PAG	16.1	40	5.6	5.3	3.6